INTERNATIONAL JOURNAL FOR NUMERICAL METHODS IN FLUIDS, VOL. 23, 47–64 (1996)

FINITE ELEMENT SOLUTIONS OF LAMINAR AND TURBULENT MIXED CONVECTION IN A DRIVEN CAVITY

SHUN-CHING LEE

Department of Mechanical Engineering, National Kaohsiung Institute of Technology, Kaohsiung, Taiwan

CHA'O-KUANG CHEN

Department of Mechanical Engineering, National Cheng-Kung University, Tainan, Taiwan

SUMMARY

This paper presents laminar and turbulent mixed convection solutions of a driven cavity flow using the finite element method. For the laminar flow, distributions of velocity and temperature with and without the effect of buoyancy force are presented and compared. For the turbulent flow, governing partial differential equations of the thermal turbulence two-equation model and kinetic turbulence two-equation model are used. Corresponding results such as kinetic eddy diffusivity, kinetic eddy energy, thermal eddy energy and their dissipations are presented.

KEY WORDS finite element; thermal turbulence; thermal eddy energy

INTRODUCTION

In forced convective flow there is an analogy between the transfer of heat and momentum and it is customary to set the turbulent Prandtl number constant in all the regions. In mixed and natural convective flows the physical mechanism of thermal eddy diffusivity is not the same as that of kinetic eddy diffusivity, so it is incorrect to assume the turbulent Prandtl number as a constant, especially in regions near the non-adiabatic wall and the turbulent core region. Gooray *et al.*[1] supposed that a bouyancy force influeces the streamline curvature and pressure strain, which can be presented by modifying the expressions of the model constant C_μ and turbulent Prandtl number σ_T. Sagara[2] introduced κ–ε models in turbulent gravity flow to calculate the Reynolds stress and Reynolds heat flux and added a buoyancy production to the source terms of the κ-equation but not the ε-equation. Humphrey and To[3] treated the Reynolds heat flux as a negative temperature gradient multiplied by ν_T/σ_T ($\sigma_T = 0{\cdot}9$) and set the buoyancy production simultaneously in both the κ- and ε-equations in mixed and natural convective flows.

In view of the above survey, there does not appear to be a general treatment that can be used for all kinds of flows and boundary conditions encountered in turbulent convection. Thus other models need to be developed that will be applicable to any turbulent flow in order to predict the Reynolds heat transfer. Since the κ–ε models are so powerful for computing kinetic eddy diffusivities, an idea to calculate the thermal eddy energy and its dissipation by two partial differential equations (i.e. κ_θ–ε_θ two-equation

CCC 0271–2091/96/010047–18

Received November 1994
Revised November 1995

models) and then to estimate the turbulent Prandtl number by a turbulence-scale model was mentioned by Arpaci and Larsen.[4] Furthermore, Newman *et al.*[5] and Chung and Sung[6] developed four-equation turbulence models to predict the turbulent boundary layer over a flat affected by buoyancy forces. This paper presents the four-equation models and applies them to two-dimensional recirculation flows.

In analysing two-dimensional turbulent flows, various wall function treaments are used to calculate the boundary conditions of kinetic eddy energy and its dissipation at a distance from the wall. In the near-wall region of mixed convective flows a buoyancy force exists which influences the velocity distributions; therefore another treatment of boundary conditions is used in this paper for the four-equation models (i.e. to set them directly at the walls).

Taylor *et al.*[7] successfully predicted turbulent flows by the finite element method. Smith[8] applied the $\kappa-\varepsilon$ model and finite element method with a coarse element mesh but encountered numerical difficulties with solution convergence. When the source term in the turbulent equations are computed in the coarse elements, it is possible to yield unreasonable values and even improper negative values, which may result in divergence. This paper applies the $\kappa-l-\varepsilon$ method[7] to mixed convection problems and checks source terms in the computing process in order to avoid unreasonable source terms and accelerate convergence.

GOVERNING EQUATIONS

With the Reynolds analogy, the Reynolds stress and Reynolds heat flux are described respectively as

$$-\overline{u_i' u_j'} = \nu_{\mathrm{T}}\left(\frac{\partial u_i}{\partial x_j} + \frac{\partial u_j}{\partial x_i}\right) - \tfrac{2}{3}\delta_{ij}\kappa, \tag{1}$$

$$-\overline{u_i' T'} = a_{\mathrm{T}}\frac{\partial T}{\partial x_i} \tag{2}$$

and the governing equations are the continuity equation

$$\frac{\partial u}{\partial x} + \frac{\partial v}{\partial y} = 0, \tag{3}$$

the x-axis directional momentum equation (the positive x-direction is set vertically upwards)

$$u\frac{\partial u}{\partial x} + v\frac{\partial u}{\partial y} = -\frac{1}{\rho}\frac{\partial}{\partial x}(p + \tfrac{2}{3}\rho\kappa) + \frac{\partial}{\partial x}\left((v + v_{\mathrm{T}})\frac{\partial u}{\partial x}\right) + \frac{\partial}{\partial y}\left((v + v_{\mathrm{T}})\frac{\partial u}{\partial y}\right) + \frac{\partial v_{\mathrm{T}}}{\partial x}\frac{\partial u}{\partial x} + \frac{\partial v_{\mathrm{T}}}{\partial y}\frac{\partial v}{\partial x} + g\beta(T - T_{\mathrm{c}}), \tag{4}$$

the y-axis directional momentum equation

$$u\frac{\partial v}{\partial x} + v\frac{\partial v}{\partial y} = -\frac{1}{\rho}\frac{\partial}{\partial y}(p + \tfrac{2}{3}\rho\kappa) + \frac{\partial}{\partial x}\left((v + v_{\mathrm{T}})\frac{\partial v}{\partial x}\right) + \frac{\partial}{\partial y}\left((v + v_{\mathrm{T}})\frac{\partial v}{\partial y}\right) + \frac{\partial v_{\mathrm{T}}}{\partial x}\frac{\partial u}{\partial y} + \frac{\partial v_{\mathrm{T}}}{\partial y}\frac{\partial v}{\partial y} \tag{5}$$

and the energy equation

$$u\frac{\partial T}{\partial x}+v\frac{\partial T}{\partial y}=\frac{\partial}{\partial x}\left((a+a_{\mathrm{T}})\frac{\partial T}{\partial x}\right)+\frac{\partial}{\partial y}\left((a+a_{\mathrm{T}})\frac{\partial T}{\partial y}\right), \tag{6}$$

where v_{T} and a_{T} can be calculated by the four-equation models.

FOUR-EQUATION MODELS

The $\kappa-\varepsilon$ equations work satisfactorily for recirculatin flows and accelerating and decelerating boundary layer flows. They are generally expressed as

$$u\frac{\partial \kappa}{\partial x}+v\frac{\partial \kappa}{\partial y}=\frac{\partial}{\partial x}\left((v+v_{\mathrm{T}})\frac{\partial \kappa}{\partial x}\right)+\frac{\partial}{\partial y}\left((v+v_{\mathrm{T}})\frac{\partial \kappa}{\partial y}\right)+v_{\mathrm{T}}G-a_{\mathrm{T}}g\beta\frac{\partial T}{\partial x}-\varepsilon, \tag{7}$$

$$u\frac{\partial \varepsilon}{\partial x}+v\frac{\partial \varepsilon}{\partial y}=\frac{\partial}{\partial x}\left[\left(v+\frac{v_{\mathrm{T}}}{1\cdot 3}\right)\frac{\partial \varepsilon}{\partial x}\right]+\frac{\partial}{\partial y}\left[\left(v+\frac{v_{\mathrm{T}}}{1\cdot 3}\right)\frac{\partial \varepsilon}{\partial y}\right]+1\cdot 44C_{\mu}\kappa G-0\cdot 7C_{\mu}\frac{\kappa}{\sigma_{\mathrm{T}}}g\beta\frac{\partial T}{\partial x}-2\cdot 0\frac{\varepsilon^2}{\kappa}, \tag{8}$$

where $G=2(\partial u/\partial x)^2+2(\partial v/\partial y)^2+(\partial u/\partial y+\partial v/\partial x)^2$ and $a_{\mathrm{T}}g\beta\partial T/\partial x$ is the buoyancy production. If the temperature is decreasing with height, the buoyancy force will increase the turbulence (i.e. the buoyancy production is positive); in contrast, if the temperature is increasing with height, the buoyancy force will decrease the turbulence (i.e. the buoyancy production is negative).

The κ_θ- and ε_θ-equations can be obtained in exactly the same way as the κ- and ε-equations. When we set a positive measure $\kappa_\theta=\frac{1}{2}(T')^2$, the governing equations become

$$u\frac{\partial \kappa_\theta}{\partial x}+v\frac{\partial \kappa_\theta}{\partial y}=\frac{\partial}{\partial x}\left((a+a_{\mathrm{T}})\frac{\partial \kappa_\theta}{\partial x}\right)+\frac{\partial}{\partial y}\left((a+a_{\mathrm{T}})\frac{\partial \kappa_\theta}{\partial y}\right)+a_{\mathrm{T}}G_\theta-\varepsilon_\theta, \tag{9}$$

$$u\frac{\partial \varepsilon_\theta}{\partial x}+v\frac{\partial \varepsilon_\theta}{\partial y}=\frac{\partial}{\partial x}\left[\left(a+\frac{a_{\mathrm{T}}}{1\cdot 3}\right)\frac{\partial \varepsilon_\theta}{\partial x}\right]+\frac{\partial}{\partial y}\left[\left(a+\frac{a_{\mathrm{T}}}{1\cdot 3}\right)\frac{\partial \varepsilon_\theta}{\partial y}\right]+0\cdot 98\frac{C_\mu}{\sigma_{\mathrm{T}}}\kappa G_\theta-\frac{\varepsilon_\theta^2}{\kappa_\theta}$$

$$+0\cdot 8\left(\frac{C_\mu}{\sigma_{\mathrm{T}}}\kappa_\theta G-\frac{C_\mu}{\sigma_{\mathrm{T}}^2}\kappa_\theta g\beta\frac{\partial T}{\partial x}\right)-0\cdot 8C_{\mathrm{D}}^{1/2}\frac{v_{\mathrm{T}}}{l_{\mathrm{m}}^2}\varepsilon_\theta, \tag{10}$$

where $G_\theta=(\partial T/\partial x)^2+(\partial T/\partial y)^2$ and the production terms in the ε_θ-equation include two parts, one coming from source terms of kinetic eddy energy and the other from source terms of thermal eddy energy. Also, we set $a_{\mathrm{T}}=v_{\mathrm{T}}/\sigma_{\mathrm{T}}$, where σ_{T} is the turbulent Prandtl number and can be inferred from scales of turbulence as follows.[4]

Employing thermal scales of turbulence in (2) and denoting θ, l_θ and u_θ as characteristic scales of temperature, length and velocity respectively, we get

$$u_\theta\theta\propto a_{\mathrm{T}}\frac{\theta}{l_\theta}\quad\text{or}\quad a_{\mathrm{T}}\propto l_\theta u_\theta. \tag{11}$$

Also, from source terms of the κ_θ-equation in the scaling of equilibrium, i.e.

$$u_\theta \theta \frac{\theta}{l_\theta} \propto \varepsilon_\theta,$$

we get

$$u_\theta \propto \frac{l_\theta \varepsilon_\theta}{\theta^2} \quad \text{or} \quad u_\theta \propto \frac{l_\theta \varepsilon_\theta}{\kappa_\theta}. \tag{12}$$

Furthermore, the dissipation of kinetic eddy energy

$$\varepsilon = C_\mu^{3/4} \frac{\kappa^{3/2}}{l_\theta}$$

gives

$$\varepsilon \propto \frac{\kappa^{3/2}}{l_\theta} \quad \text{or} \quad l_\theta \propto \frac{\kappa^{3/2}}{\varepsilon}. \tag{13}$$

Substituting (12) and (13) into (11) gives

$$a_\mathrm{T} \propto \frac{\varepsilon_\theta \kappa^3}{\kappa_\theta \varepsilon^2} = \frac{\varepsilon_\theta \kappa}{\kappa_\theta \varepsilon} \frac{\kappa^2}{\varepsilon} \tag{14}$$

and we now define the turbulent Prandtl number as

$$\sigma_\mathrm{T} = \frac{\varepsilon \kappa_\theta}{\kappa \varepsilon_\theta}. \tag{15}$$

In order to reduce the number of iterations and to increase stability, the dissipation terms in (7)–(10) are expressed respectively as

$$\varepsilon = C_\mathrm{D}^{1/2} \frac{v_\mathrm{T}}{l_\mathrm{m}^2} \kappa, \qquad \frac{\varepsilon^2}{\kappa} = C_\mathrm{D}^{1/2} \frac{v_\mathrm{T}}{l_\mathrm{m}^2} \varepsilon, \qquad \varepsilon_\theta = C_\mathrm{D}^{1/2} \frac{a_\mathrm{T}}{l_\mathrm{m}^2} \kappa_\theta, \qquad \frac{\varepsilon_\theta^2}{\kappa_\theta} = C_\mathrm{D}^{1/2} \frac{a_\mathrm{T}}{l_\mathrm{m}^2} \varepsilon_\theta. \tag{16}$$

For a wall-bounded flow such as the driven cavity flow considered in this paper, some of the model constants are modified as

$$C_\mu = 0{\cdot}09 \exp\left(-\frac{2{\cdot}5}{1 + R_\mathrm{T}/50}\right), \tag{17}$$

$$C_2 = 2{\cdot}0[1 - 0{\cdot}3 \exp(-R_\mathrm{T}^2)], \tag{18}$$

where $R_\mathrm{T} = \kappa^2/v\varepsilon$.

DECIDING ON BOUNDARY CONDITIONS

In forced convection flows, boundary conditions of κ, ε, κ_θ and ε_θ are generally set at a distance from the wall and determined via the existence of an equilibrium region between the fully turbulent region and the viscous sublayer. In mathematical terms the equilibrium occurs when the total value of the source terms of the governsing equation is zero (i.e. the production of turbulence is equal to the dissipation of turbulence). In mixed and natural convection flows we can simply set boundary conditions on the walls; for example, one can add $-2\nu(\partial\kappa^{1/2}/\partial n)^2$ into the κ-equation and set $\kappa = 0$ and $\varepsilon = 0$ on the wall,[4] where n is the co-ordinate normal to the wall, or directly set $\kappa = 0$ and $\varepsilon = -2\nu(\partial\kappa^{1/2}/\partial n)^2$ on the wall.[3] The latter treatment is used in this paper. Similarly, let $\kappa_\theta = 0$ and $\varepsilon_\theta = 2a(\partial\kappa_\theta^{1/2}/\partial n)^2$ on the constant temperature wall or $\varepsilon_\theta = 0$ on the adiabatic wall.

PROBLEM STATEMENT

Consider a driven capacity flow with positive x-direction vertically upwards as in Figure 1. The reference pressure $(p + \frac{2}{3}\rho\kappa = 0)$ is set at the centre of the region and other boundary conditions are set as follows.

(i) On the driven wall ($y = 0$) the buoyancy force has the maximum effect and aids the fluid in the direction of the driven wall velocity, so there is very thin and negligible viscous sublayer. We can treat these phenomena as a Couette flow[4] and set boundary conditions directly on the wall:

$$u = u_0, \qquad v = 0, \qquad T = T_H \quad (\phi = 1),$$

$$\kappa = C_\mu^{-1/2}\tau_w, \qquad \varepsilon = \frac{\tau_w^{3/2}}{l} \qquad \kappa_\theta = C_\mu^{-1/2}q_w, \qquad \varepsilon_\theta = \frac{\tau_w^{1/2}q_w}{l},$$

where $\phi = (T - T_C)/(T_H - T_C)$. Taylor *et al.*[7] and Smith[8] set the equilibrium region at about 2% characteristic length away from the wall to calculate the reattaching point of recirculation. For the driving and buoyancy effect, 1% is set in this paper and the mixing length l of equilibrium becomes $0{\cdot}01\kappa'H$, where κ' and H are the mixing length constant of 0·41 and the width of the flow region respectively.

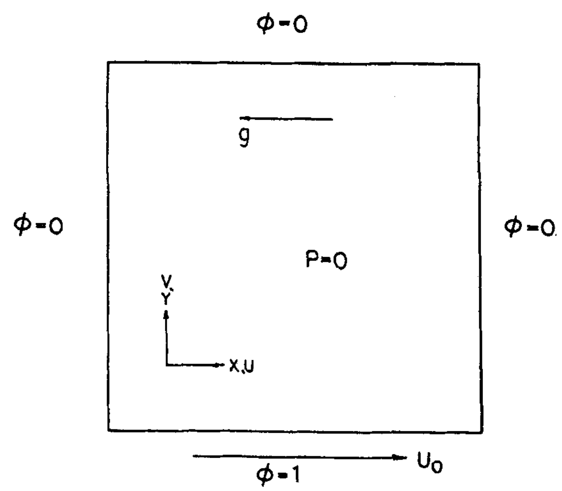

Figure 1. Scheme of a driven cavity flow region with width H and length H

(ii) On the other three walls ($x = 0, x = H$ and $y = H$)

$$u = 0, \qquad v = 0, \qquad T = T_C \quad (\phi = 0),$$

$$\kappa = 0, \qquad \varepsilon = 2v\left(\frac{\partial \kappa^{1/2}}{\partial n}\right)^2, \qquad \kappa_\theta = 0, \qquad \varepsilon_\theta = 2a\left(\frac{\partial \kappa_\theta^{1/2}}{\partial n}\right)^2.$$

NUMERICAL METHOD

This work divides the flow region into 100 or 144 elements. Solutions of laminar flow with forced and mixed convections and turbulent flow with mixed convection are calculated. For laminar flows the Galerkin weighted residual finite element formulations of governing equations are the same as those of Lee *et al.*,[9,10] while for turbulent flows they need to be modified as follows. (a) For the continuity equation

$$\sum_1^{n^e} \int_{\Omega^e} M_l\left(\frac{\partial N_j}{\partial x}u_j + \frac{\partial N_j}{\partial y}v_j\right) d\Omega^e = 0, \tag{19}$$

where M_l and N_j are four- and eight-node shape functions respectively. (b) For the x-axis directional momentum equation

$$\sum_1^{n^e} \int_{\Omega^e} \left(N_iN_ku_k\frac{\partial N_j}{\partial x}u_j + N_iN_kv_k\frac{\partial N_j}{\partial y}u_j + \frac{N_i}{\rho}\frac{\partial M_l}{\partial y}p_l + \frac{\partial N_i}{\partial x}(v+v_T)\frac{\partial N_j}{\partial x}u_j + \frac{\partial N_i}{\partial y}(v+v_T)\frac{\partial N_j}{\partial y}u_j\right.$$

$$\left. - N_i\frac{\partial v_T}{\partial x}\frac{\partial N_j}{\partial x}u_j - N_i\frac{\partial v_T}{\partial y}\frac{\partial N_j}{\partial x}v_j - g\beta N_i(N_jT_j - T_C)\right) d\Omega^e - \int_\Gamma N_i(v+v_T)\frac{\partial N_j}{\partial n}u_j\, d\Gamma = 0, \tag{20}$$

where $v_T = N_k(v_T)_k$ and $(v_T)_k = (C_\mu^{1/4} l \kappa^{1/2})_k$. (c) For the y-axis directional momentum equation

$$\sum_1^{n^e} \int_{\Omega^e} \left(N_iN_ku_k\frac{\partial N_j}{\partial x}v_j + N_iN_kv_k\frac{\partial N_j}{\partial y}v_j + \frac{N_i}{\rho}\frac{\partial M_l}{\partial y}p_l + \frac{\partial N_i}{\partial x}(v+v_T)\frac{\partial N_j}{\partial x}v_j + \frac{\partial N_i}{\partial y}(v+v_T)\frac{\partial N_j}{\partial y}v_j\right.$$

$$\left. - N_i\frac{\partial v_T}{\partial x}\frac{\partial N_j}{\partial y}u_j - N_i\frac{\partial v_T}{\partial y}\frac{\partial N_j}{\partial y}v_j\right) d\Omega^e - \int_\Gamma N_i(v+v_T)\frac{\partial N_j}{\partial n}v_j\, d\Gamma = 0. \tag{21}$$

(d) For the energy equation

$$\sum_1^{n^e} \int_{\Omega^e} \left(N_iN_ku_k\frac{\partial N_j}{\partial x}T_j + N_iN_kv_k\frac{\partial N_j}{\partial y}T_j + \frac{\partial N_i}{\partial x}(a+a_T)\frac{\partial N_j}{\partial x}T_j + \frac{\partial N_i}{\partial y}(a+a_T)\frac{\partial N_j}{\partial y}T_j\right) d\Omega^e$$

$$- \int_\Gamma N_i(v+v_T)\frac{\partial N_j}{\partial n}v_j\, d\Gamma = 0. \tag{22}$$

Similarly, the four equations of the turbulence model can be deduced as (e) the equation of kinetic eddy energy

$$\sum_1^{n^e}\int_{\Omega^e}\left(N_iN_ku_k\frac{\partial N_j}{\partial x}\kappa_j+N_iN_kv_k\frac{\partial N_j}{\partial y}\kappa_j+\frac{\partial N_i}{\partial x}(v+v_T)\frac{\partial N_j}{\partial x}\kappa_j+\frac{\partial N_i}{\partial y}(v+v_T)\frac{\partial N_j}{\partial y}\kappa_j+C_\mu^{1/2}N_i\frac{v_T}{l^2}N_j\kappa_j\right)d\Omega^e$$

$$-\int_\Gamma N_i(v+v_T)\kappa_j\,d\Gamma$$

$$=\sum_1^{n^e}\int_{\Omega^e}N_i\left[v_T\left(2\left(\frac{\partial N_k}{\partial x}u_k\right)^2+2\left(\frac{\partial N_k}{\partial y}v_k\right)^2+\left(\frac{\partial N_k}{\partial y}u_k+\frac{\partial N_k}{\partial x}v_k\right)^2\right)-a_Tg\beta\frac{\partial T}{\partial x}\right]d\Omega^e, \tag{23}$$

where $l=C_\mu^{3/4}(\kappa^{3/2}/\varepsilon)_kN_k$, (f) the equation of dissipation of kinetic eddy energy

$$\sum_1^{n^e}\int_{\Omega^e}\left(N_iN_ku_k\frac{\partial N_j}{\partial x}\varepsilon_j+N_iN_kv_k\frac{\partial N_j}{\partial y}\varepsilon_j+\frac{\partial N_i}{\partial x}\left(v+\frac{v_T}{1\cdot 3}\right)\frac{\partial N_j}{\partial x}\varepsilon_j+\frac{\partial N_i}{\partial y}\left(v+\frac{v_T}{1\cdot 3}\right)\frac{\partial N_j}{\partial y}\varepsilon_j+2C_\mu^{1/2}N_i\frac{v_T}{l^2}N_j\varepsilon_j\right)d\Omega^e$$

$$-\int_\Gamma N_i\left(v+\frac{v_T}{1\cdot 3}\right)\frac{\partial N_j}{\partial n}\varepsilon_j\,d\Gamma$$

$$=\sum_1^{n^e}\int_{\Omega^e}\left\{1\cdot 44C_\mu N_iN_k\kappa_k\left[2\left(\frac{\partial N_k}{\partial x}u_k\right)^2+2\left(\frac{\partial N_k}{\partial y}v_k\right)^2+\left(\frac{\partial N_k}{\partial y}u_k+\frac{\partial N_k}{\partial x}v_k\right)^2\right]-0\cdot 7C_\mu N_iN_k\kappa_k\frac{g\beta}{\sigma_T}\frac{\partial T}{\partial x}\right\}d\Omega^e, \tag{24}$$

(g) the equation of thermal eddy energy

$$\sum_1^{n^e}\int_{\Omega^e}\left(N_iN_ku_k\frac{\partial N_j}{\partial x}\kappa_{\theta,j}+N_iN_kv_k\frac{\partial N_j}{\partial y}\kappa_{\theta,j}+\frac{\partial N_i}{\partial x}(a+a_T)\frac{\partial N_j}{\partial x}\kappa_{\theta,j}+\frac{\partial N_i}{\partial y}(a+a_T)\frac{\partial N_j}{\partial y}\kappa_{\theta,j}\right.$$

$$\left.-C_\mu^{1/2}N_i\frac{a_T}{l^2}N_j\kappa_{\theta,j}\right)d\Omega^e-\int_\Gamma N_i(a+a_T)\frac{\partial N_j}{\partial n}\kappa_{\theta,j}\,d\Gamma$$

$$=\sum_1^{n^e}\int_{\Omega^e}N_ia_T\left[\left(\frac{\partial N_k}{\partial x}T_k\right)^2+\left(\frac{\partial N_k}{\partial y}T_k\right)^2\right]d\Omega^e \tag{25}$$

and (h) the equation of dissipation of thermal eddy energy

$$\sum_1^{n^e}\int_{\Omega^e}\left(N_iN_ku_k\frac{\partial N_j}{\partial x}\varepsilon_{\theta,j}+N_iN_kv_k\frac{\partial N_j}{\partial y}\varepsilon_{\theta,j}+\frac{\partial N_i}{\partial x}\left(a+\frac{a_T}{1\cdot 3}\right)\frac{\partial N_j}{\partial x}\varepsilon_{\theta,j}+\frac{\partial N_i}{\partial y}\left(a+\frac{a_T}{1\cdot 3}\right)\frac{\partial N_j}{\partial y}\varepsilon_{\theta,j}\right.$$

$$\left.+C_\mu^{1/2}N_i\frac{v_T}{l^2}\left(\frac{1}{\sigma_T}+0\cdot 8\right)N_j\varepsilon_{\theta,j}\right)d\Omega_e-\int_\Gamma N_i\left(a+\frac{a_T}{1\cdot 3}\right)\frac{\partial N_j}{\partial n}\varepsilon_{\theta,j}\,d\Gamma$$

$$=\sum_1^{n^e}\int_{\Omega^e}N_i\left\{0\cdot 98\frac{C_\mu}{\sigma_T^2}N_k\kappa_k\left[\left(\frac{\partial N_k}{\partial x}T_k\right)^2+\left(\frac{\partial N_k}{\partial y}T_k\right)^2\right]\right.$$

$$\left.+0\cdot 8\frac{C_\mu}{\sigma_T}\left[2\left(\frac{\partial N_k}{\partial x}u_k\right)^2+2\left(\frac{\partial N_k}{\partial y}v_k\right)^2+\left(\frac{\partial N_k}{\partial y}u_k+\frac{\partial N_k}{\partial x}v_k\right)^2\right]N_k\kappa_{\theta,k}\right\}d\Omega^e. \tag{26}$$

Combining the four governing equations, i.e. (19)–(22), the matrix equation can be expressed as

$$\tilde{A}_1\tilde{\lambda}_1 = \tilde{B}_1, \tag{27}$$

where

$$\lambda_{1,j} = \begin{bmatrix} u_j \\ p_l \\ v_j \\ T_j \end{bmatrix}.$$

The elements of the matrix $\tilde{A}_1$ are

$$a_{1,ij} = \sum_1^{n^e} \int_{\Omega^e} \begin{bmatrix} C_{11} & C_{12} & C_{13} & C_{14} \\ C_{21} & 0 & C_{23} & 0 \\ C_{31} & C_{32} & C_{33} & 0 \\ 0 & 0 & 0 & C_{44} \end{bmatrix} \mathrm{d}\Omega^e$$

$$- \int_{\Gamma^e} \begin{bmatrix} (v+v_{\mathrm{T}})N_i\partial N_j/\partial n & 0 & 0 & 0 \\ 0 & 0 & 0 & 0 \\ 0 & 0 & (v+v_{\mathrm{T}})N_i\partial N_j/\partial n & 0 \\ 0 & 0 & 0 & (a+a_{\mathrm{T}})N_i\partial N_j/\partial n \end{bmatrix} \mathrm{d}\Gamma^e,$$

where

$$C_{11} = N_iN_ku_k\frac{\partial N_j}{\partial x} + N_iN_kv_k\frac{\partial N_j}{\partial y} + (v+v_{\mathrm{T}})\left(\frac{\partial N_i}{\partial x}\frac{\partial N_j}{\partial x} + \frac{\partial N_i}{\partial y}\frac{\partial N_j}{\partial y}\right) - N_i\frac{\partial v_{\mathrm{T}}}{\partial x}\frac{\partial N_i}{\partial x},$$

$$C_{12} = \frac{N_i}{\rho}\frac{\partial M_l}{\partial x}, \qquad C_{13} = -N_i\frac{\partial v_{\mathrm{T}}}{\partial y}\frac{\partial N_j}{\partial x}, \qquad C_{14} = -N_ig\beta N_j,$$

$$C_{21} = M_l\frac{\partial N_j}{\partial x}, \qquad C_{23} = M_l\frac{\partial N_j}{\partial y}, \qquad C_{31} = -N_i\frac{\partial v_{\mathrm{T}}}{\partial x}\frac{\partial N_j}{\partial y}, \qquad C_{32} = \frac{N_i}{\rho}\frac{\partial M_l}{\partial y},$$

$$C_{33} = N_iN_ku_k\frac{\partial N_j}{\partial x} + N_iN_kv_k\frac{\partial N_j}{\partial y} + (v+v_{\mathrm{T}})\left(\frac{\partial N_i}{\partial x}\frac{\partial N_j}{\partial x} + \frac{\partial N_i}{\partial y}\frac{\partial N_j}{\partial y}\right) - N_i\frac{\partial v_{\mathrm{T}}}{\partial y}\frac{\partial N_j}{\partial y},$$

$$C_{44} = N_iN_ku_k\frac{\partial N_j}{\partial x} + N_iN_kv_k\frac{\partial N_j}{\partial y} + (a+a_{\mathrm{T}})\left(\frac{\partial N_i}{\partial x}\frac{\partial N_j}{\partial x} + \frac{\partial N_i}{\partial y}\frac{\partial N_j}{\partial y}\right).$$

The elements of the vector $\tilde{B}_1$ are

$$b_{1,i} = \sum_1^{n^e} \int_{\Omega^e} \begin{bmatrix} -N_ig\beta T_{\mathrm{C}} \\ 0 \\ 0 \\ 0 \end{bmatrix} \mathrm{d}\Omega^e + \int_{\Gamma^e} \begin{bmatrix} (v+v_{\mathrm{T}})N_i\partial u/\partial n \\ 0 \\ (v+v_{\mathrm{T}})N_i\partial v/\partial n \\ (a+a_{\Gamma})N_i\partial T/\partial n \end{bmatrix} \mathrm{d}\Gamma^e.$$

Since the four equations of the turbulence model, i.e. (23)–(26), do not need to be calculated simultaneously, the matrix equation can be written in common as

$$\tilde{A}_2\tilde{\lambda}_2 = \tilde{B}_2, \tag{28}$$

where

$$\lambda_{2,j} = [\phi_j].$$

The elements of the matrix $\tilde{A}_2$ are

$$a_{2,ij} = \sum_1^{n^e} \int_{\Omega^e} [C_{11}]\,\mathrm{d}\Omega^e,$$

where in the κ-equation $\phi_j = \kappa_j$ and

$$C_{11} = N_i N_k u_k \frac{\partial N_j}{\partial x} + N_i N_k v_k \frac{\partial N_j}{\partial y} + (v + v_\mathrm{T})\left(\frac{\partial N_i}{\partial x}\frac{\partial N_j}{\partial x} + \frac{\partial N_i}{\partial y}\frac{\partial N_j}{\partial y}\right) + C_\mu^{1/2} N_i \frac{v_\mathrm{T}}{l^2} N_j,$$

in the ε-equation $\phi_j = \varepsilon_j$ and

$$C_{11} = N_i N_k u_k \frac{\partial N_j}{\partial x} + N_i N_k v_k \frac{\partial N_j}{\partial y} + \left(v + \frac{v_\mathrm{T}}{1\cdot 3}\right)\left(\frac{\partial N_i}{\partial x}\frac{\partial N_j}{\partial x} + \frac{\partial N_i}{\partial y}\frac{\partial N_j}{\partial y}\right) + 2\cdot 0 C_\mu^{1/2} N_i \frac{v_\mathrm{T}}{l^2} N_j,$$

in the κ_θ-equation $\phi_j = \kappa_{\theta,j}$ and

$$C_{11} = N_i N_k u_k \frac{\partial N_j}{\partial x} + N_i N_k v_k \frac{\partial N_j}{\partial y} + \left(a + \frac{a_\mathrm{T}}{1\cdot 3}\right)\left(\frac{\partial N_i}{\partial x}\frac{\partial N_j}{\partial x} + \frac{\partial N_i}{\partial y}\frac{\partial N_j}{\partial y}\right) + C_\mu^{1/2} N_i \frac{a_\mathrm{T}}{l^2} N_j$$

and in the ε_θ-equation $\phi_j = \varepsilon_{\theta,j}$ and

$$C_{11} = N_i N_k u_k \frac{\partial N_j}{\partial x} + N_i N_k v_k \frac{\partial N_j}{\partial y} + \left(a + \frac{a_\mathrm{T}}{1\cdot 3}\right)\left(\frac{\partial N_i}{\partial x}\frac{\partial N_j}{\partial x} + \frac{\partial N_i}{\partial y}\frac{\partial N_j}{\partial y}\right) + C_\mu^{1/2} N_i \frac{v_\mathrm{T}}{l^2}\left(\frac{1}{\sigma_\mathrm{T}} + 0\cdot 8\right) N_j.$$

The elements of the vector $\tilde{B}_2$ are

$$b_i = \sum_1^{n^e} \int_{\Omega^e} [b_1]\,\mathrm{d}\Omega^e,$$

where in the κ-equation

$$b_1 = N_i\left\{v_\mathrm{T}\left[2\left(\frac{\partial N_k}{\partial x}u_k\right)^2 + 2\left(\frac{\partial N_k}{\partial y}v_k\right)^2 + \left(\frac{\partial N_k}{\partial y}u_k + \frac{\partial N_k}{\partial x}v_k\right)^2\right] - a_\mathrm{T} g\beta \frac{\partial N_k}{\partial x} T_k\right\},$$

in the ε-equation

$$b_1 = N_k\left\{1\cdot 44 C_\mu N_k \kappa_k\left[2\left(\frac{\partial N_k}{\partial x}u_k\right)^2 + 2\left(\frac{\partial N_k}{\partial y}v_k\right)^2 + \left(\frac{\partial N_k}{\partial y}u_k + \frac{\partial N_k}{\partial x}v_k\right)^2\right] + 0\cdot 7 C_\mu \frac{g\beta}{\sigma_\mathrm{T}} N_k \kappa_k \frac{\partial N_k}{\partial x} T_k\right\},$$

in the κ_θ-equation

$$b_1 = N_i a_\mathrm{T}\left[\left(\frac{\partial N_k}{\partial x}T_k\right)^2 + \left(\frac{\partial N_k}{\partial y}T_k\right)^2\right]$$

and in the ε_θ-equation

$$b_1 = N_i\left\{0{\cdot}98\frac{C_\mu}{\sigma_T^2}N_k\kappa_k\left[\left(\frac{\partial N_k}{\partial x}T_k\right)^2+\left(\frac{\partial N_k}{\partial y}T_k\right)^2\right]\right.$$

$$\left.+0{\cdot}8\frac{C_\mu}{\sigma_T}\left[2\left(\frac{\partial N_k}{\partial x}u_k\right)^2+2\left(\frac{\partial N_k}{\partial y}v_k\right)^2+\left(\frac{\partial N_k}{\partial y}u_k+\frac{\partial N_k}{\partial x}v_k\right)^2+\frac{g\beta}{\sigma_T}\frac{\partial N_k}{\partial x}T_k\right]N_k\kappa_{\theta,k}\right\}.$$

The frontal method is used in solving the matrix equation; if successive solutions ϕ_n and ϕ_{n+1} satisfy the criterion

$$\frac{|\phi_{n+1}-\phi_n|_{\max}}{|\phi_{n+1}|_{\max}}\leqslant 10^{-3},$$

the iteration stops and solutions ϕ_{n+1} are treated as convergent solutions. The solution process is as follows.

1. Solve the matrix equation (27) iteratively and determine $u_{n+1}, p_{n+1}, v_{n+1}$ and T_{n+1}. A laminar flow solution is finished at this step. For turbulent flows the mixing length distribution can be predicted at the first iteration by

$$l = 0{\cdot}29\sqrt{\left[\left(\frac{|\mathrm{d}u/\mathrm{d}y|}{|\mathrm{d}^2u/\mathrm{d}y^2|}\right)^2+\left(\frac{|\mathrm{d}v/\mathrm{d}x|}{|\mathrm{d}^2v/\mathrm{d}x^2|}\right)^2\right]}.$$

2. Solve the κ-equation iteratively and derive κ_{n+1} (initially set the turbulent Prandtl number to 1·0).
3. Solve the ε-, κ_θ- and ε_θ-equations respectively and non-iteratively and derive $\varepsilon_{n+1}, \kappa_{\theta,n+1}$ and $\varepsilon_{\theta,n+1}$.
4. Update

$$l_{n+1} = 0{\cdot}5\left(l_n + C_\mu\frac{\kappa^{3/2}}{\varepsilon}\right).$$

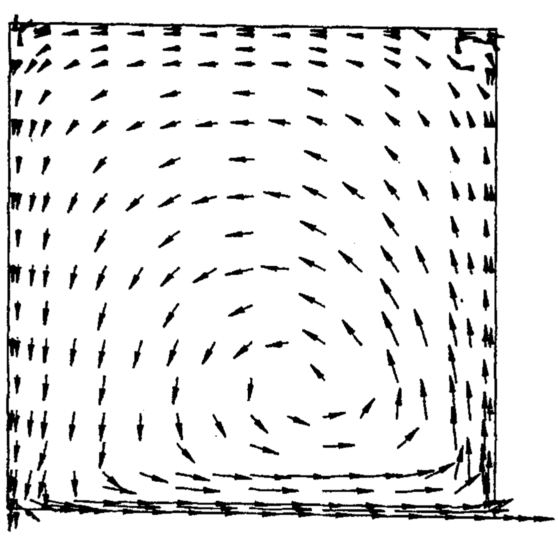

Figure 2. Dimensionless velocity distribution of laminar forced convectin with $Re = 10^2$

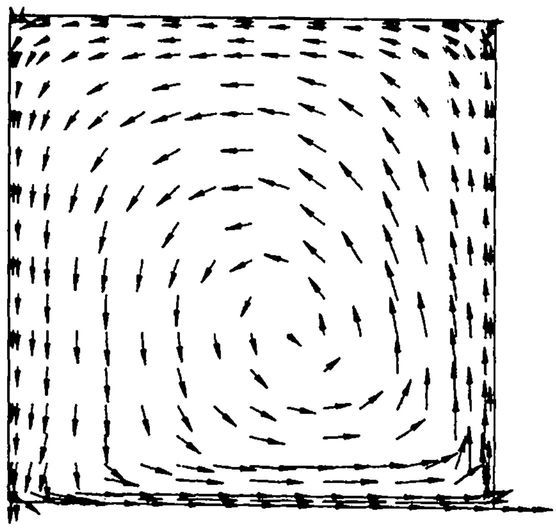

Figure 3. Dimensionless velocity distribution of laminar mixed convection with $Re = 10^2$ and $Gr/Re^2 = 1{\cdot}0$

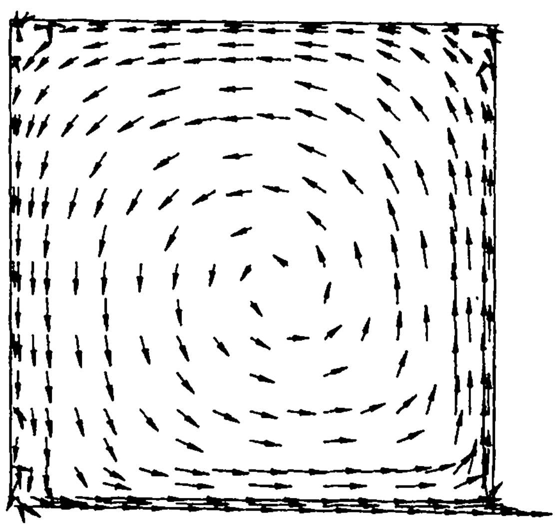

Figure 4. Dimensionless velocity distribution of turbulent mixed convection with $Re = 10^4$ and $Gr/Re^2 = 0{\cdot}1$

5. Update

$$\sigma_{\mathrm{T},n+1} = 0{\cdot}5\left(\sigma_{\mathrm{T},n} + \frac{\varepsilon\kappa_\theta}{\kappa\varepsilon_\theta}\right).$$

6. Return to step 1 until solutions converge.

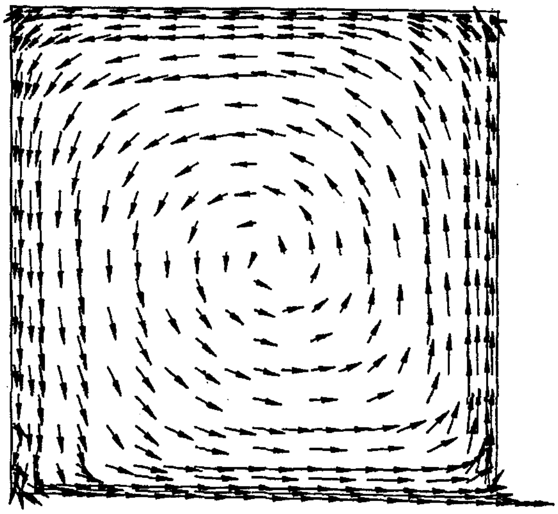

Figure 5. Dimensionless velocity distribution of turbulent mixed convection with $Re = 10^4$ and $Gr/Re^2 = 1{\cdot}0$

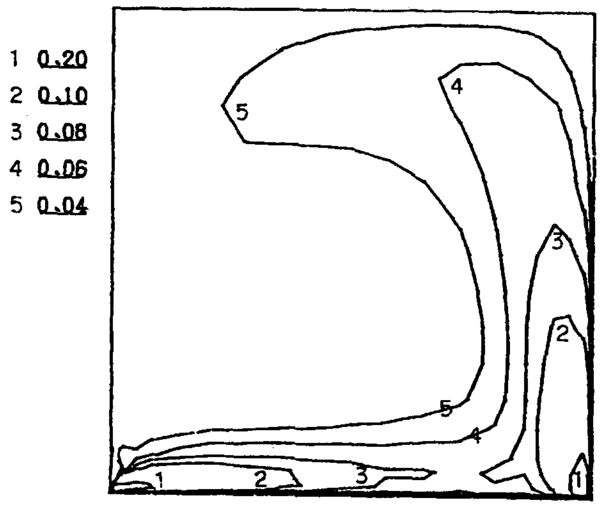

Figure 6. Dimensionless kinetic eddy energy of turbulent mixed convection with $Re = 10^4$ and $Gr/Re^2 = 0{\cdot}1$

RESULTS AND DISCUSSION

Figures 2 and 3 present velocity distributions of laminar forced and mixed convection respectively. Figures 4 and 5 present velocity distributions of turbulent mixed convection. In laminar flows, as seen in Figures 2 and 3, the centre of recirculation is close to the driven wall for forced convection and is transported to the centre of the flow region for mixed convection. In turbulent flows, as seen in Figures 4 and 5, the centre of recirculation is just the centre of the flow region.

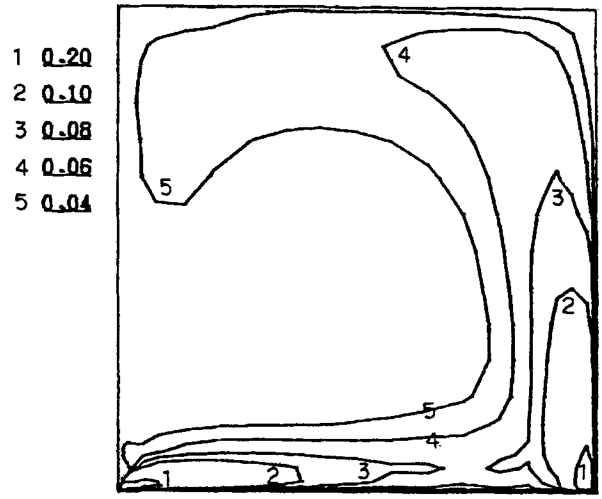

Figure 7. Dimensionless kinetic eddy energy of turbulent mixed convection with $Re = 10^4$ and $Gr/Re^2 = 1{\cdot}0$

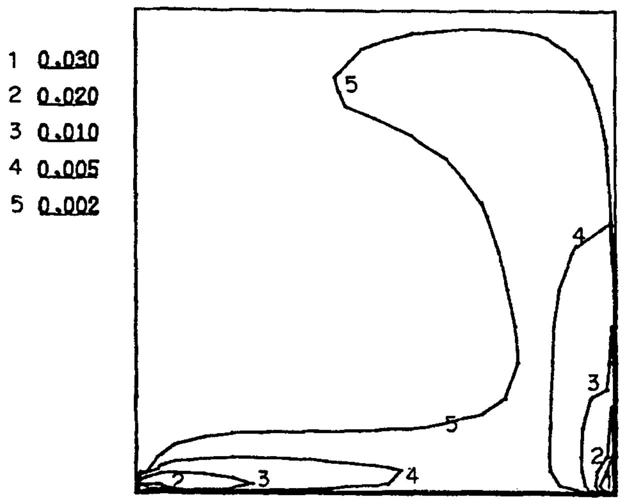

Figure 8. Dimensionless dissipation kinetic eddy energy of turbulent mixed convection with $Re = 10^4$ and $Gr/Re^2 = 0{\cdot}1$

Figures 6 and 7 present distributions of kinetic eddy energy. The maximum occurs near the driven wall for large velocity gradient. The driven wall is a source for inducing turbulence and the turbulence is transmitted along the streamlines. Of course, the buoyancy force helps in transmitting the turbulence, as seen by comparing Figures 6 and 7. The same phenomena were found for its dissipation and the kinetic eddy diffusivity; therefore only results for $Gr/Re^2 = 0{\cdot}1$ are shown in Figures 8 and 9.

Figures 10 and 11 present temperature distributions of laminar forced and mixed convection respectively. Figures 12 and 13 present temperature distributions of turbulent mixed convection. In laminar flows, as seen in Figures 10 and 11, the temperature distribution is slightly influenced by the buoyancy force. In turbulent flows, as seen in Figures 12 and 13, the buoyancy force apparently

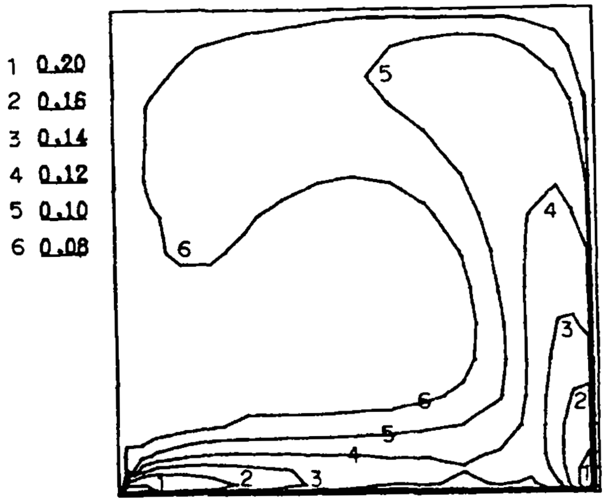

Figure 9. Dimensionless eddy viscosity of turbulent mixed convection with $Re = 10^4$ and $Gr/Re^2 = 0{\cdot}1$

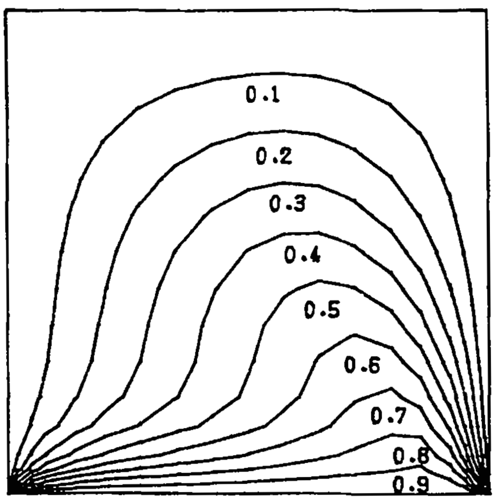

Figure 10. Dimensionless temperature distribution of laminar forced convection with $Re = 10^2$

decreases the temperature at the centre of the flow region. Also, temperature distributions of turbulent flows are very different from those of laminar flows, the former being a circulating type and the latter a diffusing type.

Figure 14 presents distributions of thermal eddy energy. The maximum occurs near the driven wall for large absolute value of the temperature gradient vector. Around the centre of the flow region the temperature gradient is zero, so the thermal energy dissipates quickly. The same phenomena are found for the dissipation of thermal eddy energy as shwon in Figure 15.

The heat transfer parameter Nu can be calculated by

$$Nu = \int_0^H \frac{a_T}{a} \frac{\partial \theta}{\partial n} \, dl$$

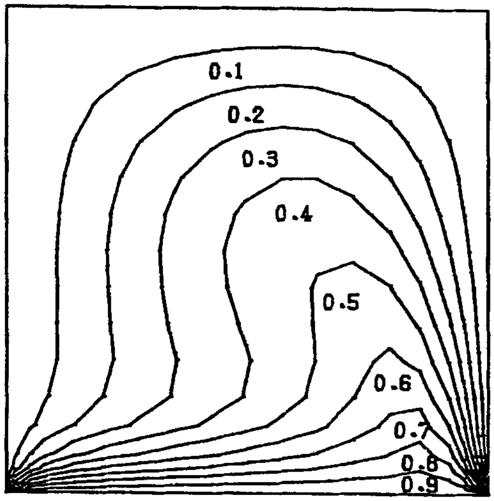

Figure 11. Dimensionless temperature distribution of laminar mixed convection with $Re = 10^2$ and $Gr/Re^2 = 1{\cdot}0$

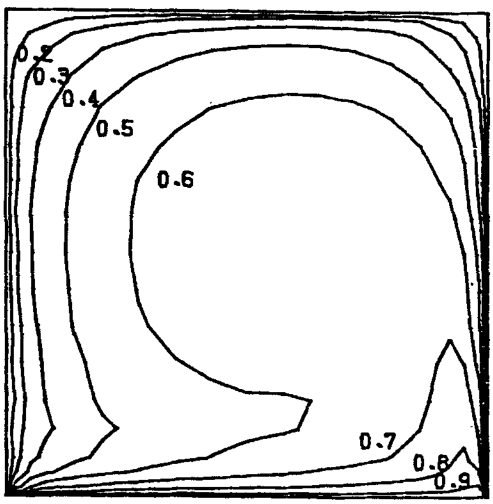

Figure 12. Dimensionless temperature distribution of turbulent mixed convection with $Re = 10^4$ and $Gr/Re^2 = 0{\cdot}1$

for the driven wall and by

$$Nu_i = \int_0^H \frac{\partial \theta}{\partial n}\, \mathrm{d}l$$

for the other three walls, where i indicates each wall and n and l are in the directions normal and tangent to the wall respectively. Results are presented in Table I. As shown in Table I, when 10 × 10 elements are used for $Re = 10^4$ and $Gr/Re^2 = 1{\cdot}0$, there is 2·4% error between $\sum Nu_i$ and Nu at $y = 0$, so 12 × 12 elements are used in this case, yielding only 0·75% error. Humphrey and To[3] computed the heat transfer rate of an open heated cavity across which fluid flows in a direction inclined at 45° to the

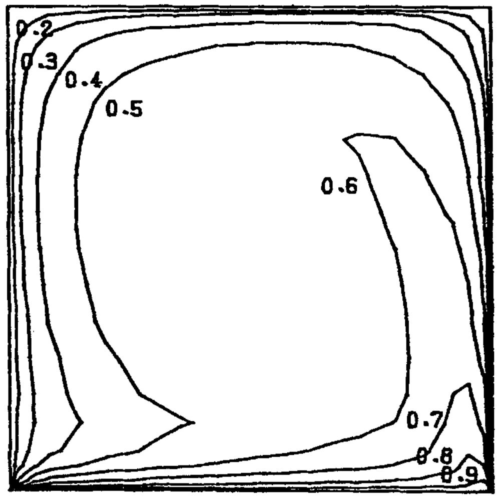

Figure 13. Dimensionless temperature distribution of turbulent mixed convection with $Re = 10^4$ and $Gr/Re^2 = 1{\cdot}0$

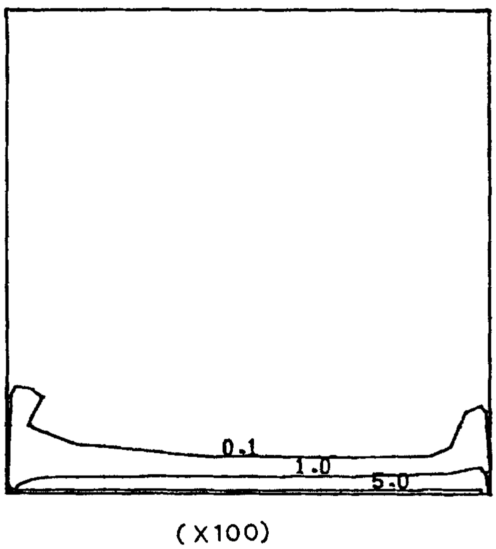

Figure 14. Dimensionless thermal energy of turbulent mixed convection with $Re = 10^4$ and $Gr/Re^2 = 1{\cdot}0$

gravity force. They stated that when the value of Re^2/Gr is large, such as $Re^2/Gr > 21{\cdot}3$, the fluid does not enter the cavity, so the problem can be treated as a driven cavity flow. According to two cases calculated with $Re^2/Gr = 0{\cdot}85$ and $21{\cdot}3$, they inferred the formula

$$Nu = 21{\cdot}16(Re^2/Gr)^{0{\cdot}43}. \tag{29}$$

However comparing data between Table I and (29), the driven cavity flow seems to be found when $Re^2/Gr > 37$ in their study.

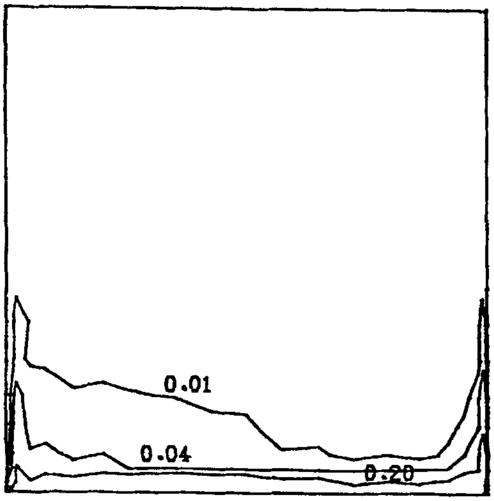

Figure 15. Dimensionless dissipation of thermal eddy energy of turbulent mixed convection with $Re = 10^4$ and $Gr/Re^2 = 1{\cdot}0$

Table I shows the buoyancy force seems to have little influence on the Nusselt number and that $Nu_{x=0} < Nu_{y=H} < Nu_{x=H} < Nu_{y=0}$ in turbulent flows whereas $Nu_{y=H} < Nu_{x=O} < Nu_{x=H} < Nu_{y=O}$ in laminar flows.

CONCLUSIONS

Finite element solutions of turbulent and laminar mixed convection flows in a driven cavity were presented. Results showed that the kinetic eddy energy and its dissipation had larger values near the driven wall. This is because the driven wall induced larger velocity gradients which enhanced the development of the kinetic eddy; then the kinetic eddy was transported and circulated around the cavity via convection. Similarly, owing to the larger temperature gradients near the heated wall, distributions of thermal eddy energy and its dissipation presented larger values near the wall. Because the order of temperature gradients in the flow region is small, the thermal eddy was dissipated rapidly and existed

Table I. Nusselt number for various convection conditions

Elements		10 × 10					12 × 12
Re		10^2			10^4		10^4
Gr/Re^2		0·0	0·1	1·0	0·1	1·0	1·0
Nu_i	$x = 0$	2·342	2·328	2·278	22·50	22·31	22·74
	$y = H$	0·453	0·504	0·763	25·32	27·23	27·50
	$x = H$	4·881	4·980	5·360	49·58	49·93	49·99
$\sum Nu_i$		7·676	7·812	8·401	97·40	99·47	100·23
Nu	$y = 0$	7·728	7·868	8·473	98·96	101·93	100·99

near the driven wall only. These physical phenomena reveal that is seems to be inadequate to treat the turbulent Prandtl number as a constant in mixed convection flow. The use of the thermal two-equation models appears beneficial in solving the flows described.

REFERENCES

1. A. M. Gooray, C. B. Watkins and W. Aung, 'A two pass procedure for the calculation of heat transfer in recirculating flow', *Numer. Heat Transfer*, **6**, 423–440 (1983).
2. K. Sagara, 'Calculation of turbulent gravity flow', *Trans. Arch. Inst. Jpn.*, 88–96 (1981).
3. J. A. C. Humphrey and W. M. To, 'Numerical simulation of buoyant turbulent flow—II. Free and mixed convection in a heated cavity', *Int. J. Heat Mass Transfer*, **29**, 593–610 (1986).
4. V. S. Arpaci and P. S. Larsen, *Convection Heat Transfer*, Prentice-Hall, London, 1984.
5. G. R. Newman, B. E. Launder and J. L. Lumley, 'Modeling the behaviour of homogeneous scalar turbulence', *J. Fluid Mech.*, **111**, 217–232 (1981).
6. M. K. Chung and H. J. Sung, 'Four-equation turbulence model for prediction of the turbulent boundary affected by buoyancy force over a flat plate', *Int. J. Heat Mass Transfer*, **27**, 2387–2395 (1984).
7. C. Taylor, C. E. Thomas and K. Morgan, 'Modeling flow over a backward-facing step using the F.E.M. and the two-equation model of turbulence', *Int. J. numer. method fluids*, **1**, 295–304 (1981).
8. R. M. Smith, 'On the finite-element calculation of turbulent flow using the κ–ε model', *Int. j. numer. method fluids*, **4**, 303–319 (1984).
9. S. C. Lee, K. L. Wong and C. K. Chen, 'The finite element solution of laminar combined convection from a horizontal cylinder', *Comput. Mechods Appl. Mech. Eng.*, **50**, 147–161 (1985).
10. K. L. Wong, S. C. Lee and C. K. Chen, 'Finite element solution of laminar combined convection from a sphere', *ASME J. Heat Transfer*, **108**, 860–865 (1986).